EC
Journals.ASM.org

Overexpression of S4D Mutant of *Leishmania donovani* ADF/Cofilin Impairs Flagellum Assembly by Affecting Actin Dynamics

Gaurav Kumar,[a] Rashmi Srivastava,[a] Kalyan Mitra,[b] Amogh A. Sahasrabuddhe,[a] and Chhitar M. Gupta[a]

Division of Molecular and Structural Biology[a] and Electron Microscopy Unit,[b] CSIR-Central Drug Research Institute, Lucknow, India

***Leishmania*, like other eukaryotes, contains large amounts of actin and a number of actin-related and actin binding proteins. Our earlier studies have shown that deletion of the gene corresponding to *Leishmania* actin-depolymerizing protein (ADF/cofilin) adversely affects flagellum assembly, intracellular trafficking, and cell division. To further analyze this, we have now created ADF/cofilin site-specific point mutants and then examined (i) the actin-depolymerizing, G-actin binding, and actin-bound nucleotide exchange activities of the mutant proteins and (ii) the effect of overexpression of these proteins in wild-type cells. Here we show that S4D mutant protein failed to depolymerize F-actin but weakly bound G-actin and inhibited the exchange of G-actin-bound nucleotide. We further observed that overexpression of this protein impaired flagellum assembly and consequently cell motility by severely impairing the assembly of the paraflagellar rod, without significantly affecting vesicular trafficking or cell growth. Taken together, these results indicate that dynamic actin is essentially required in assembly of the eukaryotic flagellum.**

Reorganization of actin cytoskeleton is central to several fundamental processes in eukaryotes, including cell division, cell shape regulation and, transmission of extracellular stimuli toward the cell interior. Such diverse functions of actin cytoskeleton have been attributed to the dynamic character of actin, which requires high turnover of actin monomers in its filamentous meshwork by a treadmilling process (11). This process is greatly facilitated by the actin-depolymerizing protein (ADF)/cofilin family of actin binding proteins (40). These proteins generally have three distinct biochemical activities, *viz.*, F-actin depolymerization, actin filament severing, and nucleotide exchange (12). By virtue of these activities, ADF/cofilins play a key role in regulating the actin dynamics and associated functions in eukaryotes (7). Functions of the actin cytoskeleton have been considered important not only in higher eukaryotes but also in several parasites that cause life-threatening human diseases, such as *Plasmodium* (5, 49), *Acanthamoeba* (10, 23), *Trypanosoma* (13, 21), *Leishmania* (30, 47), and others.

Leishmania spp. constitute a group of medically important protozoan parasites that are responsible for a vast array of devastating human diseases, including kala-azar (visceral leishmaniasis). These organisms exist in two morphobiological forms, amastigotes (inside the human host) and promastigotes (in the insect vector), which undergo extensive cytoskeletal rearrangement during their transformation from one form to the other (25). The promastigote form possesses a single highly motile protruding flagellum, which drives the cell to move forward, whereas the rudimentary flagellum in amastigotes has been considered important to establish host-parasite interactions (22). Further, a direct involvement of the promastigote flagellum has been demonstrated in sandfly infection (16). Apart from being important for parasite biology, the *Leishmania* flagellum has also been considered a good model system to study the biology of flagella and cilia in connection with ciliopathies in humans (4, 22).

The *Leishmania* flagellum is comprised of two main structural components, the axoneme and the paraflagellar rod (PFR). Whereas the axoneme powers beating in most eukaryotic flagella (44), the PFR has been implicated in flagellar motility and wave-form generation (42). All eukaryotic flagella are microtubule-based dynamic structures, which utilize the microtubule-based motor proteins, kinesins and dyneins, for trafficking proteins from the base to the tip and *vice versa* in a process called intraflagellar transport (IFT) during their assembly and disassembly (recently reviewed in reference 28). Although there are several studies which have shown the presence of actin and actin binding proteins in the flagellar compartment (19, 31, 32, 34, 47, 52, 55, 57), their role in the assembly and functions of the flagellum has not yet been fully explored.

Our previous studies have shown that besides containing actin (LdACT), *Leishmania donovani* parasites also contain a homolog of ADF/cofilin (LdCof), not only in their cell bodies but also in the flagella (47, 52). It has further been shown that knockout of the LdCof gene in *Leishmania* promastigotes results in short, stumpy, and nonmotile cells with shorter and paralyzed flagella (52). Additionally, it has been reported that in LdCof null mutants, most of the actin was present in the form of bundles, suggesting a possible role of LdCof-mediated actin dynamics in assembly of the flagellum. To further investigate this, we have now created LdCof mutants in which the serine-4 residue was replaced with aspartate (S4D) or alanine (S4A) and have analyzed the effects of their overexpression in wild-type cells. In addition, we expressed these mutant proteins in bacteria and, after their purification and characterization, analyzed their biochemical properties in terms of actin binding, actin depolymerization, and exchange of actin-bound nucleotides. Our results revealed that overexpression of the S4D

Received 9 January 2012 **Accepted** 20 March 2012
Published ahead of print 6 April 2012
Address correspondence to Chhitar M. Gupta, drcmg@rediffmail.com.
This article is no. 8232 from CSIR-CDRI, Lucknow, India.
Supplemental material for this article may be found at http://ec.asm.org/.

doi:10.1128/EC.00013-12

mutant of LdCof impairs the assembly of the *Leishmania* flagellum by altering the actin dynamics in wild-type cells.

MATERIALS AND METHODS

Cell culture and transfections. *Leishmania donovani* cells were maintained in high-glucose Dulbecco modified Eagle medium (DMEM) supplemented with 10% heat-inactivated fetal bovine serum and 40 μg/ml gentamicin at 25°C. *Leishmania* promastigotes were transfected by electroporation (52) and plated on DMEM agar plates containing 20 μg/ml tunicamycin (a nucleoside antibiotic required for selection of cells transfected with p6.5MCS plasmid for constitutive expression of recombinant proteins in *Leishmania*). Independent colonies were picked and cultured in liquid medium (DMEM with appropriate additives). *L. tarentolae* T7/TR cells (Jena Biosciences, Germany) were maintained in brain heart infusion broth containing hemin (0.0005%, wt/vol), penicillin-streptomycin (5 units penicillin/100 ml and 5 μg streptomycin/100 ml), and two other antibiotics, nourseothricin (NTC) and hygromycin, at 100 μg/ml.

DNA constructs and proteins. Forward primers were designed to replace serine-4 (S4) with aspartate (D) or alanine (A) in the *LdCof* gene (52), whereas reverse primers contained a hexahistidine tag in frame. The PCR-amplified products were subcloned in pET21d (Novagen) and p6.5MCS (kind gifts from K. P. Chang, Rosalind Franklin University of Medicine and Science) expression vectors for expression in bacteria and *Leishmania*, respectively, and were designated as S4D and S4A genes. These clones were sequenced by the dideoxy chain termination method to confirm the mutations that were introduced in the *LdCof* gene.

LdCof and the mutant proteins, S4D and S4A, were expressed in BL21(DE3) Rosetta strain (Novagen) and purified to homogeneity, as described earlier (52). Purified proteins were subjected to N-terminal sequencing to reconfirm the replacement of S4 by D or A. Purified proteins were analyzed by circular dichroism and fluorimetry to ensure the gross structural identity (results not shown).

Rabbit skeletal muscle actin was purified from rabbit muscle acetone powder as described previously (41) and stored in lyophilized form at −80°C after addition of sucrose (2 mg/mg protein). G-actin was subjected to size exclusion chromatography each time after a new frozen vial was thawed, and only the peak fractions of monomeric actin were used in the experiments. To prepare ADP.actin monomers, ATP.actin was first polymerized and then dialyzed thoroughly against G-actin buffer (5 mM Tris-Cl, 0.2 mM $CaCl_2$, 0.5 mM dithiothreitol [DTT], and 0.2 mM NaN_3, pH 8.0) containing 0.5 mM ADP and 80 μM $MgCl_2$. To replace ADP by N^6-etheno-ATP (ε-ATP) (Molecular Probes) on actin monomers, the actin polymer pellets were resuspended in G-actin buffer containing 0.5 mM ε-ATP and the nucleotide exchange was allowed to take place for 24 h at 4°C in the dark. Excess ε-ATP was removed by exchanging the medium with G-actin buffer containing 30 μM ε-ATP by repeatedly passing through a 30-kDa-cutoff Centricon filter (Millipore). To prepare ε-ADP.G-actin, ε-ATP.G-actin was polymerized, and the pellets obtained after ultracentrifugation were dialyzed in G-actin buffer containing 30 μM ε-ATP and 80 μM $MgCl_2$. All G-actin preparations were ultracentrifuged to remove any insoluble material prior to experimentation. ε-ATP/ε-ADP labeled actin preparations were stored on ice in the dark and used within 24 h.

Leishmania donovani actin (LdACT) was expressed and purified using a *Leishmania tarentolae*-based inducible expression system (Jena Biosciences, Germany). The *L. donovani* actin gene (47) was cloned in pLexsy-I ble vector (Jena Biosciences, Germany) at NcoI and KpnI restriction sites to have a hexahistidine tag (His_6) at its C terminus. The LdACT clone thus obtained was transfected by electroporation in *L. tarentolae* strain T7/TR (Jena Biosciences) and selected with 100 μg/ml bleomycin along with NTC and hygromycin according to the instructions of the manufacturer. Clones were selected by plating transfected cells on brain heart infusion (BHI) agar plates and subcultured in BHI broth containing appropriate additives. One of the expressing clones was used throughout for expression and purification of LdACT. For expression, 200 ml BHI broth was first inoculated with 20 ml of a 48-h-grown culture and then allowed to grow further for 48 h with mild shaking (60 rpm) at 26°C. Protein expression was induced by addition of 10 μg/ml tetracycline. Cells were harvested after 24 h of induction by centrifugation and washed once with chilled phosphate-buffered saline, pH 7.4 (PBS), containing 0.5% (wt/vol) glucose. The cells were lysed in lysis buffer (PBS containing 0.2 mM $MgCl_2$, 0.5 mM ATP, 1%[vol/vol] Triton X-100, and protease inhibitors) on ice for 30 min. The lysate was briefly sonicated to reduce viscosity and centrifuged at 20,000 × *g* for 20 min at 4°C, and the cleared lysate was passed through an Ni-nitrilotriacetic acid (Ni-NTA) fast-flow matrix (Qiagen). The matrix was washed with 50 column volumes of lysis buffer containing 20 mM imidazole, and LdACT was eluted in lysis buffer containing 200 mM imidazole. The eluted LdACT was dialyzed in G-actin buffer for 48 h with one buffer replacement at an interval of 24 h. Dialyzed proteins were concentrated using Centricon (Millipore) and ultracentrifuged at 100,000 × *g* for 40 min to remove any insoluble material.

F-actin binding and depolymerization. F-actin sedimentation assay of rabbit muscle actin (actin) and *Leishmania donovani* actin (LdACT) was carried out as described previously (52) in the presence or absence of LdCof, S4D, or S4A protein. The supernatants and the pellets were adjusted to the same volume and analyzed by 12% SDS-PAGE. After staining with Coomassie brilliant blue R-250, gels were scanned and band densities were quantified using ImageMaster software (Amersham Pharmacia).

Actin pulldown assay. Actin monomer binding with LdCof, S4D, or S4A protein was assessed by actin pulldown assay as described previously (52). Briefly, ADP.G-actin (5 μM) was incubated separately with various concentrations of LdCof, S4D, and S4A proteins for 1 h at room temperature. The reaction mixture was mixed with Ni-NTA superflow beads (Qiagen) and centrifuged briefly to sediment the bead-bound proteins. After thorough washing of the beads with G-actin buffer containing 0.5 mM ADP, bead-bound proteins were eluted using 100 mM EDTA in G-actin buffer. The eluates were analyzed by 12% SDS-PAGE to assess the binding of LdCof and its mutants with ADP.G-actin.

Binding of LdCof, S4D, and S4A proteins with LdACT was assessed by using lysates of an LdCof null mutant ($LdCof^{-/-}$) (52). The cells were lysed by sonication in G-actin buffer containing 0.5 mM ADP and protease inhibitor cocktail (Sigma), and clear supernatants were collected after centrifugation at 100,000 × *g* for 1 h at 4°C. The lysate was pretreated with Ni-NTA beads and then incubated with various concentrations of LdCof, S4D, and S4A proteins for 1 h on ice. Supernatants and bead-bound proteins were separated as described above, and LdACT contents in different fractions were analyzed by Western blotting using anti-LdACT antibodies. Band intensities of Coomassie blue-stained gels or Western blots were quantified using ImageMaster software (Amersham Pharmacia).

Nucleotide exchange assay. Exchange of actin-bound nucleotide under steady-state polymeric conditions was performed as described previously (12) with slight modification. Briefly, ε-ATP.G-actin was polymerized for 2 h by addition of KCl (50 mM), $MgCl_2$ (2 mM), and ε-ATP (30 mM). The F-actin (20 μM) thus obtained was incubated separately with 20 μM each of LdCof, S4D, or S4A protein for 20 min at room temperature, and the nucleotide exchange was assessed by monitoring the rate of fluorescence decrease (λ_{ex} = 350 nm; λ_{em} = 410 nm) at 25°C immediately after addition of ATP (1 mM). Similarly, nucleotide exchange on G-actin was measured by incubating ε-ADP.G-actin (20 μM) with an equimolar amount of LdCof, S4D, or S4A protein for 20 min in G-actin buffer. The decrease in fluorescence was monitored after addition of a chase amount of ATP, as described above. In control reactions, the decrease in fluorescence was monitored in the absence of LdCof, S4D, or S4A protein after addition of 1 mM ATP.

Transmission electron microscopy. For transmission electron microscopy, cells were washed once with chilled phosphate-buffered saline (PBS) and fixed in 4% paraformaldehyde (freshly prepared) containing 1% glutaraldehyde in PBS for 1 h at room temperature. After repeated washings with PBS, the cells were postfixed with 1% OsO_4 in PBS at room

temperature for 2 h and encapsulated in 2% low-melting-point agarose (Sigma). Samples were stained *en bloc* with 1% aqueous uranyl acetate, dehydrated in an ascending series of ethanol mixtures, embedded in Epon-Araldite plastic mixture, and polymerized at 60°C for 24 h. Ultrathin sections (50 to 70 nm) were picked up onto 200-mesh copper grids and were doubly stained with uranyl acetate and lead citrate. Sections were analyzed under a FEI Tecnai-12 Twi transmission electron microscope equipped with a SIS Mega View II charge-coupled-device (CCD) camera at 80 kV (FEI Co.).

Antibodies, Western blotting, and immunofluorescence. Monospecific polyclonal antibodies to LdCof and LdACT were generated as described earlier (47, 52). Anti-α/β-tubulin antibodies were procured from Sigma. Anti-His rabbit polyclonal antibodies were obtained from Santa Cruz Biotechnology. Anti-PFR monoclonal antibody (MAb) 2E10 was a kind gift from Diane McMahon Pratt (Yale University). Lysates of *L. donovani* expressing LdCof, S4D, or S4A protein as well as wild-type cells were prepared by resuspending and boiling the cell pellets for 5 min in 1× SDS sample buffer. Samples were resolved by SDS-PAGE (12% resolving gel) and electroblotted onto nitrocellulose membrane (Pall). LdCof, S4D, or S4A protein and actin were detected using anti-LdCof and anti-LdACT antibodies, respectively. Blots were developed by using chemiluminescence substrate (Millipore), and signals were collected on X-ray films (GE Healthcare).

Immunofluorescence microscopy was performed as described previously (52). Briefly, cultured *Leishmania* cells were washed two times with chilled PBS containing 0.5% (wt/vol) glucose and settled on poly-L-lysine coated glass coverslips for 5 min. Adhered cells were fixed with 4% freshly prepared paraformaldehyde solution in PBS for 30 min at room temperature and then permeabilized using 1% (vol/vol) Triton X-100 in PBS containing 0.05% (wt/vol) glycine. Coverslips were then treated with blocking solution (0.5% fish gelatin [Sigma] in PBS) to block nonspecific interactions with antibodies in subsequent incubations. LdACT, PFR, and α/β-tubulin were probed with their respective antibodies diluted in blocking solution. Overexpression of LdCof, S4D, or S4A protein was probed with anti-His rabbit polyclonal antibody. All the antibody incubations, including those with secondary fluorophore-tagged antibodies, were carried out at 4°C in the dark with rocking for 4 h. Coverslips were mounted on fluorescent mounting medium (Merck) and stored at 4°C in the dark until analysis. Images were captured on a Zeiss LSM510 Meta confocal microscope using a 63x 1.4-numerical-aperture (NA) (oil) Plan Apochromat lens. Images were processed and merged for presentation using Adobe Photoshop version 7.0.

RESULTS

Replacement of serine-4 by aspartate results in inhibition of exchange of actin-bound nucleotide by LdCof. *Leishmania* parasites express a homolog of ADF/cofilin, LdCof, which has high F-actin-depolymerizing activity but only weak F-actin-severing activity (52). Importantly, LdCof shows nucleotide exchange in steady-state F-actin solutions, suggesting its involvement in maintaining a high actin monomer pool by treadmilling. Since phosphorylation of serine-3/4 has been shown to inactivate ADF/cofilins (3, 6) and this residue is conserved in LdCof also, we created LdCof mutants by replacing serine-4 with an aspartate residue (S4D), which imitates phosphorylated serine, and with an alanine residue (S4A), which cannot be phosphorylated, and then analyzed the effects of these mutations on the actin dynamics. These mutants were expressed in bacteria, purified to homogeneity, and characterized by sequencing the first 10 N-terminal amino acid residues. The actin-depolymerizing activity of the mutants was assessed by sedimentation assay (41). Consistent with our previous observation (52), LdCof depolymerized both the rabbit muscle actin and LdACT effectively, whereas under identical conditions, the S4D mutant completely failed to depolymerize any of these two actins. Interestingly, S4A protein showed only limited actin depolymerization activity (~50%) (Fig. 1). Since the binding affinity of LdCof for ADP.actin was high compared to that for ATP.actin (52), we assessed the binding affinities of S4D and S4A proteins with the ADP.actin monomers. The binding of both S4D and S4A proteins with the rabbit muscle ADP.actin was very weak at all concentrations compared to that of LdCof; however, it was significant with LdACT (Fig. 2). To further characterize the interactions of S4D and S4A proteins with actin, we also ascertained the ability of LdCof and its mutants to accelerate nucleotide exchange on rabbit muscle actin. Since the mutant proteins have shown differential actin depolymerization and monomer binding activi-

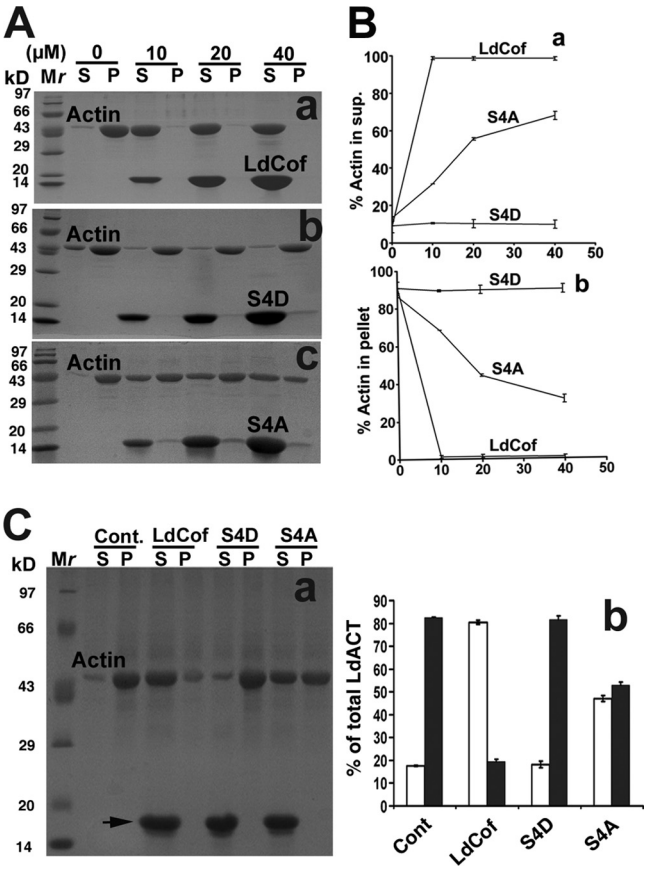

FIG 1 Depolymerization of rabbit muscle actin (actin) and *Leishmania donovani* actin (LdACT) by LdCof, S4D, and S4A proteins. (A) Depolymerization of rabbit muscle actin (5 μM) by LdCof, S4D, and S4A proteins at various concentrations. Coomassie blue-stained SDS-PAGE of supernatant (S) and pellet (P) fractions is shown. LdCof protein (a), unlike S4D protein (b), depolymerized F-actin, whereas S4A protein (c) showed limited F-actin depolymerization. Mr, molecular mass markers. (B) Quantitative analysis of F-actin depolymerization by LdCof, S4D, and S4A proteins at various concentrations in supernatants (a) and pellets (b). Values are expressed as percentages of total actin and are means from three independent experiments ± standard deviations. (C) Panel a, depolymerization of LdACT (5 μM) by LdCof, S4D, and S4A proteins, each at 40 μM. Coomassie blue-stained SDS-PAGE of supernatant (S) and pellet (P) fractions is shown. LdCof, unlike S4D protein, depolymerized F-actin, whereas S4A protein showed limited F-actin depolymerization. Panel b, quantitative analysis of LdACT depolymerization by LdCof, S4D, and S4A proteins. Values are expressed as percentages of total actin and are means from three independent experiments ± standard deviations. Open bar, monomeric LdACT; solid bar, polymeric LdACT; Cont., control; M*r*, molecular weight markers.

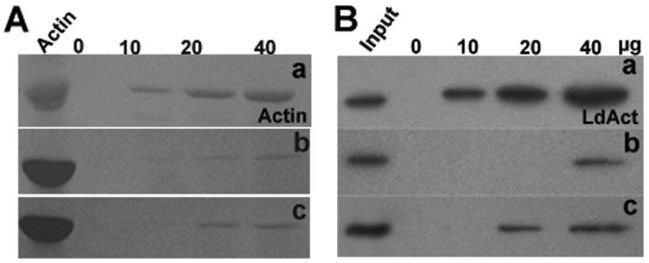

FIG 2 (A) Binding of actin monomers (5 μM) at various concentrations of LdCof (a), S4D (b), and S4A (c) proteins. Coomassie blue-stained SDS-PAGE of ADP.actin bound to Ni-NTA beads is shown. (B). Binding of LdCof (a), S4D (b), and S4A (c) with LdACT monomers in lysates of LdCof null mutants (1.6 mg protein/ml) at various concentrations. Western blot analysis of bead-bound LdACT using anti-LdACT antibodies is shown.

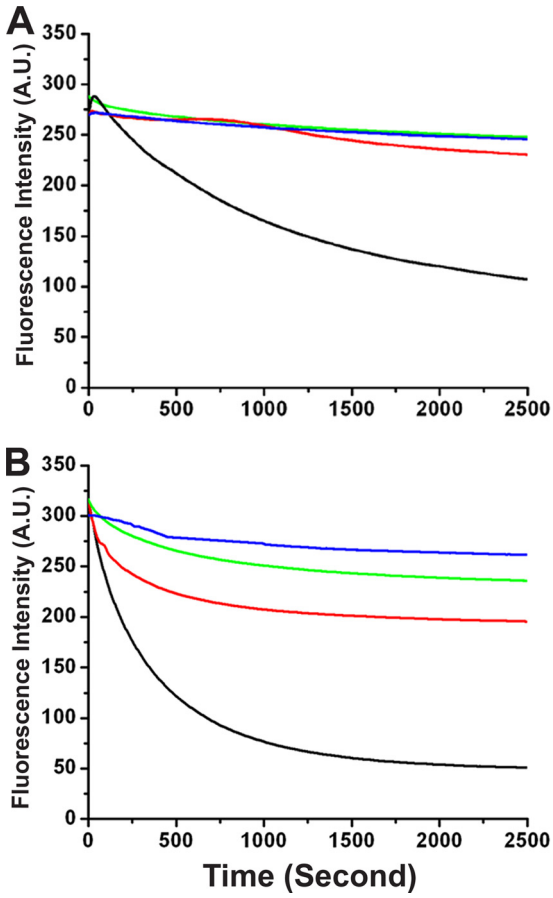

FIG 3 (A) Nucleotide exchange under steady-state polymeric conditions of actin (20 μM) with 20 μM each of LdCof, S4D, and S4A proteins. The nucleotide exchange was assessed by monitoring the rate of fluorescence decrease (λ_{ex} = 350 nm; λ_{em} = 410 nm) at 25°C immediately after the addition of ATP (1 mM). (B) Nucleotide exchange on G-actin (20 μM) with 20 μM each of LdCof, S4D, and S4A proteins. The nucleotide exchange was assessed by monitoring the rate of fluorescence decrease (λ_{ex} = 350 nm; λ_{em} = 410 nm) at 25°C immediately after the addition of ATP (1 mM). Blue, control; black, LdCof; green, S4D; red, S4A.

ties (Fig. 1 and 2), nucleotide exchange activity in both the steady-state F-actin and monomeric ADP.actin solutions was measured. In the steady-state F-actin solution, S4D protein completely failed to show any nucleotide exchange, whereas S4A protein exhibited only marginal activity. As nucleotide exchange cannot take place in the polymeric state of actin (40), these results are consistent with the actin depolymerization capacities of the mutants (Fig. 3A). Unlike in the steady state, in the monomeric ADP.actin solutions, S4D protein inhibited spontaneous nucleotide exchange, whereas S4A protein accelerated the exchange, though to a limited extent, compared to LdCof (Fig. 3B). Together, these results indicated that the N terminus of the LdCof, specifically serine-4, plays a crucial role in regulating the actin dynamics in *Leishmania* cells.

Overexpression of S4D protein results in generation of a short flagellar phenotype by altering the actin dynamics in wild-type *Leishmania* promastigotes. LdCof has been implicated in regulation of multiple cellular events in *Leishmania*, such as flagellum elongation, paraflagellar rod (PFR) assembly (52), flagellar pocket duplication, intracellular vesicular trafficking, and the cell cycle (51). In principle, LdCof possesses two major biochemical activities akin to those of ADF/cofilin proteins (40), *viz.*, F-actin depolymerization and nucleotide exchange activities. However, it was not clear how these biochemical activities of LdCof could affect the diverse cellular processes in *Leishmania* cells. Since S4D mutant protein failed to depolymerize F-actin but weakly bound monomeric ADP.LdACT and inhibited the nucleotide exchange on actin monomers, we overexpressed this protein to analyze the functional consequences of inhibition of the exchange of actin-bound nucleotide in wild-type *Leishmania* promastigotes. All three proteins, *viz.*, LdCof, S4D, and S4A, were overexpressed ≥20-fold as judged by SDS-PAGE analysis followed by Western blotting using anti-LdCof antibodies (Fig. 4A). At least 8 independent clones of S4D protein overexpressing *Leishmania* promastigotes were analyzed for protein expression and morphological aberrations (see Fig. S1 in the supplemental material), and one of these clones was analyzed in detail. Although the overexpression of LdCof or S4A protein in the wild-type cells led to significant ($P < 0.0001$) shortening of the length of their flagella (wild type, 13.12 ± 1.40 μm; LdCof overexpressing, 9.97 ± 2.03 μm; S4A protein overexpressing, 8.35 ± 1.51 μm [n = 100]), it did not significantly affect their cell body length and motility (wild-type motility, ~96%; LdCof overexpressing, ~ 90%; S4A overexpressing, ~90%) (Fig. 5). However, the cells that overexpressed S4D protein were largely stumpy (94.9% ± 3%) and immotile and possessed considerably short flagella (2.96 ± 0.74 μm; n = 100) (Fig. 5). In order to assess whether these phenotypic effects were due to some differences in the intracellular distributions of the overexpressed proteins, the cells were labeled with anti-His_6 antibodies and then analyzed by immunofluorescence microscopy (Fig. 4B). The S4D and S4A proteins, similarly to the native protein, were distributed throughout the cell body, including the nucleus and flagellum, in the overexpressing cells.

As S4D protein-overexpressing cells were morphologically similar to the LdCof gene knockout mutants, in which PFR was absent (52), we analyzed the presence of the PFR in the S4D protein-overexpressing cells by both immunofluorescence microscopy and immunoblotting using MAb 2E10 (a kind gift of Diane McMahon Pratt, Yale University), which is known to selectively react with the two major *Leishmania* PFR proteins, *viz.*, PFR1 and PFR2 (29). Whereas the flagella of the wild-type, LdCof-overexpressing, and S4A protein-overexpressing cells were intensely

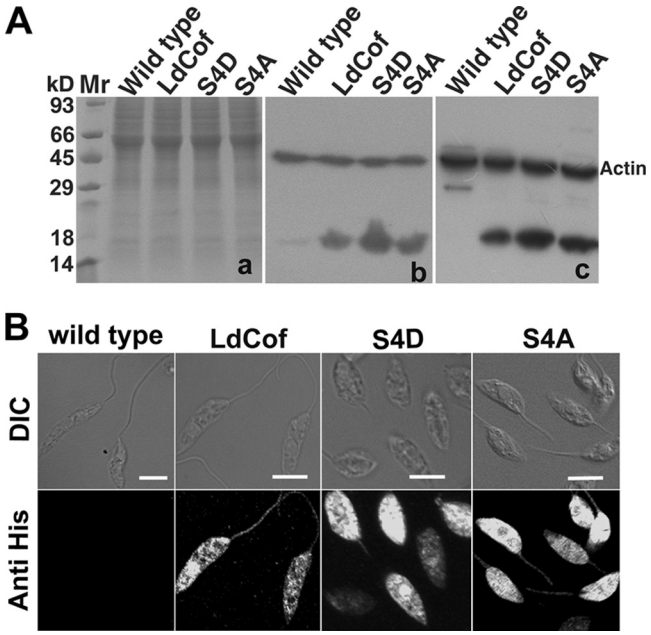

FIG 4 (A) SDS-PAGE analysis showing overexpression of LdCof, S4D, and S4A proteins in *Leishmania donovani* cells. Panel a, Coomassie blue-stained 12% SDS-PAGE of total cell lysates showing equal loading of samples. Panel b, Western blot of panel a using polyclonal rabbit anti-LdCof antibodies, which detected a specific protein band of about 17 kDa in total cell lysates, and polyclonal rabbit anti-*Leishmania* actin antibodies for detection of actin as a loading control. Panel c, Western blot of panel a using polyclonal rabbit anti-His antibodies for detection of overexpressed proteins and polyclonal rabbit anti-*Leishmania* actin antibodies for detection of actin as a loading control. Mr, molecular mass markers. (B) Intracellular distribution of overexpressed LdCof, S4D, and S4A proteins in *L. donovani* promastigotes analyzed by immunofluorescence microscopy, using rabbit anti-His antibodies. The S4D and S4A proteins, similarly to the native protein, are distributed throughout the cell body, including the nucleus and flagellum, in the overexpressing cells. Wild-type cells were used as control. Bar, 5 μm.

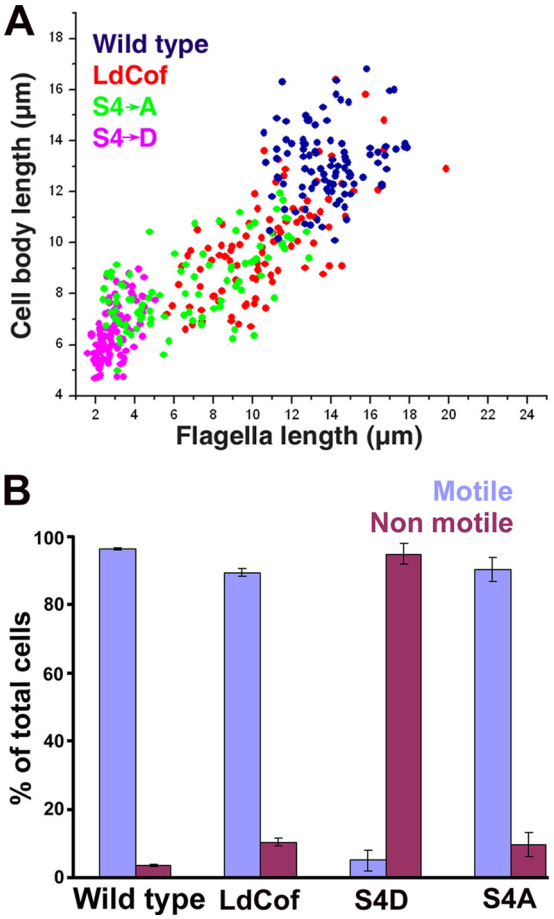

FIG 5 (A) Analysis of flagellar length versus body length of wild-type cells (blue) and LdCof (red), S4D (pink), and S4A (green) protein-overexpressing cells. A total of 100 cells were analyzed in each case. (B) Analysis of percentages of motile and nonmotile cells among wild-type cells and LdCof, S4D, and S4A protein-overexpressing cells. A total of 100 cells in each case were counted. Values are expressed as percentages of the total number of cells and are means from three independent experiments ± standard deviations.

stained by MAb 2E10, the cells that overexpressed S4D protein remained completely unstained (Fig. 6A), suggesting a loss of PFR proteins in these cells. This was strongly supported by our failure to detect these proteins in the whole-cell lysates of the S4D protein-overexpressing cells by immunoblotting (Fig. 6B). The observed complete absence of PFR proteins in the whole-cell lysates could primarily be due to their rapid degradation in the cytoplasm, which has also been suggested by earlier investigators (2, 36). To further confirm the loss of the PFR assembly in S4D protein-overexpressing cells, we analyzed about 20 transverse and longitudinal sections each of the LdCof, S4D-, and S4A protein-overexpressing cells along with the wild-type cells by transmission electron microscopy (Fig. 7A). Unlike the LdCof and S4A protein-overexpressing cells, which showed the PFR structure continuously running along the axoneme, almost all (>90%) of the cells that overexpressed S4D protein were devoid of such a structure. Besides, similarly to the ADF/cofilin and myosin XXI gene knockout mutants (33, 52), S4D protein-overexpressing cells also did not show any residual PFR structure or the fibers that link the axoneme to the PFR, which are seen prominently in the PFR gene knockout mutants (36) under the transmission electron microscope.

Since, based on the results of our *in vitro* studies (Fig. 1 to 3), overexpression of S4D protein is expected to reduce the actin dynamics in cells, we analyzed the frequency of occurrence of the filament-like structures in the wild-type and S4D protein-overexpressing cells along with the LdCof heterozygous (LdCof $^{+/-}$) and homozygous (LdCof $^{-/-}$) mutants. For this, first the cells were labeled with anti-*Leishmania* coronin antibodies, as described by us earlier (39), and then the number of cells that contained actin filament-like structures of 2 μm or greater in length were counted. A total of five fields, with each field containing at least 30 cells, were examined in each case (Fig. 7B). Based on this analysis, significantly more S4D protein-overexpressing (23.96% ± 6.41%), LdCof$^{+/-}$ (31.28% ± 9.30%), and LdCof$^{-/-}$ (91.30% ± 3.79%) cells than wild-type cells (16.39% ± 2.38%) showed filament-like structures.

Intracellular actin distribution and vesicular trafficking in S4D protein-overexpressing cells. In *Leishmania* cells, actin is diffusely distributed throughout the cell body, including the flagellum, kinetoplast, and nucleus, and sometimes shows filament bundles and patches (30, 47). However, upon complete ablation of LdCof in these cells, most of actin accumulates in the form of

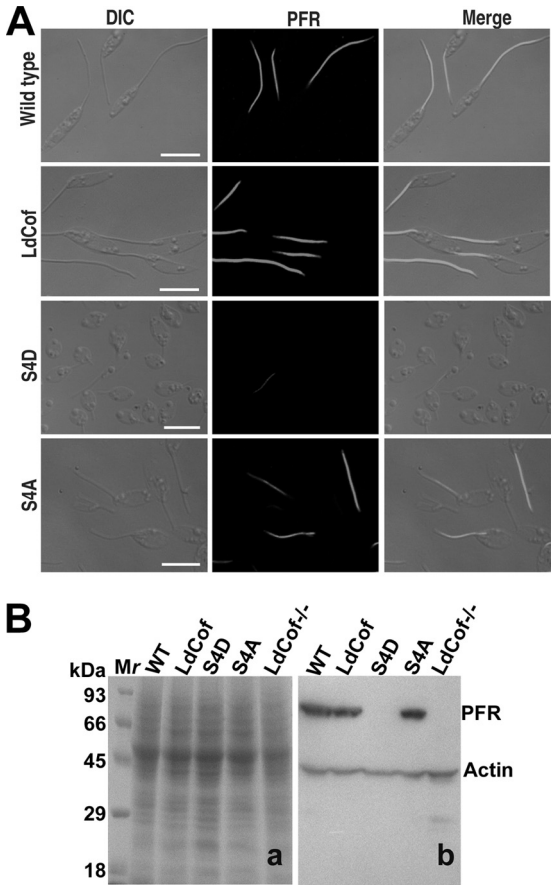

FIG 6 (A) Analysis of PFR assembly in LdCof, S4D, and S4A protein-overexpressing cells. Cells were processed for immunofluorescence analysis as described in Materials and Methods. PFR1 and PFR2 proteins were stained with MAb 2E10. The immunofluorescence images showed that S4D protein-overexpressing cells were largely negative for PFR staining, whereas both the LdCof and S4A protein-overexpressing cells were positively stained. Bar, 5 μm. (B) Western blot analysis of the major PFR protein (PFR1 and PFR2) expression in S4D-overexpressing cells. Panel a, Coomassie blue-stained polyvinylidene difluoride membrane; panel b, Western blot of panel a using MAb 2E10 antibody. Anti-*Leishmania* actin antibodies were used to stain actin as the internal loading control.

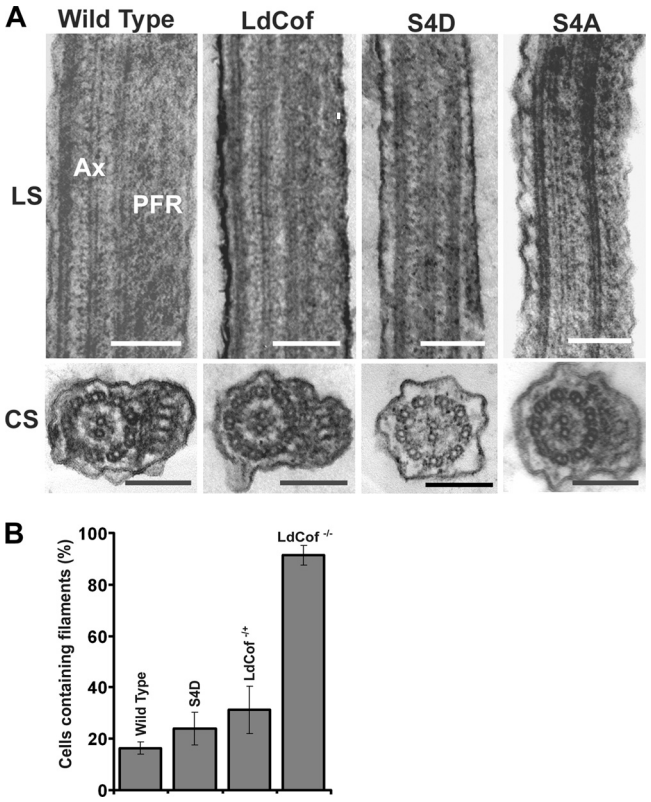

FIG 7 (A) Transmission electron micrographs of thin sections of flagella from chemically fixed whole cells, showing the absence of PFR in S4D protein-overexpressing cells. Longitudinal sections (LS) of the flagella show the axoneme (AX) and PFR confined between the axoneme and the flagellar membrane in wild-type and LdCof, S4D, and S4A protein-overexpressing cells. Bar, 200 nm. Cross sections (CS) of the flagellum show the presence of PFR in wild-type and LdCof and S4A protein-overexpressing cells and the complete absence of this structure in the CS of the S4D protein-overexpressing promastigotes. Bar, 200 nm. (B) Quantification of numbers of cells containing filament-like structures after labeling with anti-coronin antibodies (39) to assess the effects of S4D protein overexpression on the frequency of the occurrence of actin filament-like structures. Values shown are means from five fields, with each field containing 30 cells. *P* values: wild type versus S4D-overexpressing cells, <0.05; wild type versus LdCof$^{+/-}$, <0.01; LdCof$^{+/-}$ versus S4D-overexpressing cells, > 0.10. *P* values were calculated using Student's *t* test.

bundles, and no actin is seen in the residual flagellum by immunofluorescence (51, 52). As the S4D protein overexpression phenotypes closely resembled those of the LdCof gene deletion mutants, we also analyzed the distribution of actin in these cells. Along with actin, the cells were also labeled for tubulin to assess the length of the flagellum axoneme. Immunofluorescence microscopy revealed that the actin distributions in S4D and S4A protein-overexpressing cells were almost the same as that in the wild-type cells (Fig. 8A). However, similarly to the case for the LdCof null mutants (52), a flagellar sleeve (membrane extension without axoneme) (17) was clearly visible beyond the length of the axoneme (stained with antitubulin antibodies) in the flagella of S4D protein-overexpressing cells. This was further confirmed by transmission electron microscopy, where a sleeve-like structure was clearly seen in at least 20% of the longitudinal sections of the flagellum (Fig. 8B).

Actin dynamics are also involved in intracellular vesicular trafficking and cell division in *Leishmania* cells (33, 51). Therefore, S4D protein-overexpressing cells were assessed for trafficking of endocytic vesicles using FM4-64 dye, which is known to be internalized by the endocytic activity and to traffic down toward the posterior pole with time (37, 48). Interestingly, vesicular trafficking remained unaffected in S4D protein-overexpressing cells (see Fig. S2 in the supplemental material), suggesting selective disturbances in the flagellar actin dynamics. As LdCof$^{+/-}$ heterozygous mutants (52) were depleted of only about 50% of the total LdCof, we also analyzed the intracellular trafficking of FM4-64 dye in these cells. Interestingly, these mutants, like S4D protein-overexpressing cells, also did not show any inhibition of the vesicular trafficking compared to that in the wild-type cells (see Fig. S2 in the supplemental material). Further, no significant differences were observed between the growth patterns of the LdCof and S4D protein-overexpressing cells (or the LdCof $^{+/-}$ mutants) (see Fig. S3 in the supplemental material). Taken together, these results indicated that S4D protein overexpression selectively affects the flagellum assembly in *Leishmania* cells.

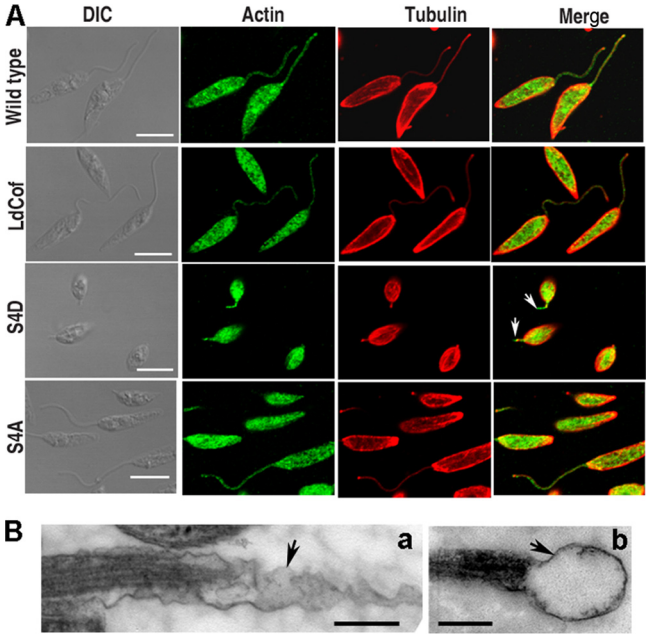

FIG 8 (A) Analysis of actin distribution and length of flagellar axoneme in LdCof, S4D, and S4A protein-overexpressing cells. In wild-type and overexpressing cells, actin and tubulin were stained with polyclonal rabbit anti-*Leishmania* actin antibodies and polyclonal mouse anti-α,β-tubulin antibodies, respectively. Actin distributions in S4D and S4A protein-overexpressing cells were similar to that in wild-type cells. A flagellar sleeve (membrane extension without axoneme [16]) was clearly visible beyond the length of the axoneme (stained with antitubulin antibodies and marked by an arrow) in the flagella of S4D protein-overexpressing cells. Bar, 5 μm. (B) Ultrastructure of flagellar sleeve (arrows) in S4D-overexpressing *Leishmania* cells by transmission electron microscopy. Elongated (a) and bulbous (b) membrane extensions beyond the axoneme extremity are seen. Bar, 200 nm.

DISCUSSION

The present study shows that the replacement of serine-4 by an aspartate residue in LdCof completely abolishes the actin-depolymerizing activity of this protein. It further shows that the S4D mutant weakly binds G-actin and inhibits the spontaneous exchange of actin-bound nucleotide. This suggests that overexpression of this protein in the wild-type cells might subtly affect the actin dynamics by competing with the native LdCof, which in turn may adversely affect the *Leishmania* cellular activities that are highly dependent on the optimal dynamics of actin. Since overexpression of S4D protein selectively affected the flagellar assembly and consequently the motility without affecting the other gross cellular activities, our results demonstrate that dynamic actin is essentially required in the assembly of the *Leishmania* flagellum.

Regulation of the flagellar length has long been a puzzle, and it has been addressed mostly by the current knowledge of the intraflagellar transport (IFT) system, which operates through the microtubule-based motor proteins (28). As the flagellar compartment does not contain any protein translation machinery, such as ribosomes, all the flagellar proteins are synthesized in the cytoplasm, assembled into protein complexes, and then transported selectively to the flagellar compartment (20, 43). In transport both "across" and "within" the flagellar compartment, only the microtubule-based transport systems have been implicated (14, 28). Interestingly, the actin cytoskeleton, which plays a key role in the intracellular trafficking, has not received its due attention despite the evidenced presence of actin and actin-binding proteins in this organelle (31, 32, 38, 47, 52, 58).

Actin has an inherent tendency to form filaments, which act as tracks for motor proteins such as myosins, forming acto-myosin motors for short-distance cargo movements in collaboration with the microtubule-based motors that are responsible for long-distance movements (24, 45, 46). As actin and myosin (myosin XXI) are freely available in both the cytoplasmic and flagellar compartments (32, 47) in *Leishmania*, they may be expected to form an acto-myosin transport system, which may play an important role in transport of the flagellar protein complexes from the cytoplasm to the flagellar base and/or across and within the flagellar compartment. Since the intracellular trafficking is not significantly influenced by the overexpression of S4D protein, we infer that perhaps the transport of these complexes across and/or within the flagellar compartments is affected in the S4D protein-overexpressing cells.

To achieve the optimal activity of the acto-myosin motors, actin filaments need to be in a highly dynamic state (15, 50, 60). Apparently, a ready pool of polymerizable actin is the key to the maintenance of the high actin dynamics. As the protein transport across the flagellar compartment has been reported to be highly selective (8, 27, 39), this may limit the transport of actin across the cytoplasm-flagellum interface. Our results show that S4D protein is very well diffusible across this interface. We therefore envisage that with a limiting amount of actin, inhibitory activity of S4D protein on actin-bound nucleotide exchange may cause a significant reduction in the polymerizable pool of actin monomers. Under such a condition, if the actin monomers do not diffuse freely from the cytoplasm to the flagellar compartment to compensate the polymerizable actin pool, alterations in the dynamics of the actin filaments would be an obvious consequence. Fitting in the hypothesis of an actin-based transport system in the flagellar compartment (33), reduced actin dynamics should affect the acto-myosin motor function, which in turn may hamper the assembly of the flagellar components. This partly explains why both the heterozygous ADF/cofilin gene knockout mutant and S4D protein-overexpressing *Leishmania* cells show short flagellar phenotypes without showing any significant effect on the intracellular vesicular trafficking, which has been reported to be significantly reduced in ADF/cofilin null and myosin XXI-depleted *Leishmania* cells (33, 52).

It is intriguing to note that the S4D protein-overexpressing cells, myosin XXI heterozygous gene knockout mutants (33), and ADF/cofilin gene deletion mutants (52) all possess small flagella without any PFR structure and the axoneme attachment fibers. In these cells the axoneme structure near the flagellar tip region also is missing, suggesting a role of the actin dynamics not only in the assembly of the PFR and the axoneme attachment fibers but also in the axoneme assembly. Defects in the axoneme assembly have also been observed in *L. mexicana* mitogen-activated protein (MAP) kinase (LmxMKK) gene deletion mutants (56). Further, LmxDH2.2 null cells have been reported to have nonemerging flagella with defective axoneme organization and no PFR (2). However, deletion of LmxMK3 (another MAP kinase) results in a short flagellar phenotype, with significant defects only in the PFR assembly (18). As the PFR assembles only on the flagellar region outside the flagellar pocket region, it may be argued that a minimum length of the axoneme is required for PFR assembly. There are two supports to this hypothesis: (i) the null mutant of SMP-1

(a flagellar membrane protein) shows a flagellar length averaging around 7 μm with fully assembled PFR (53), and (ii) about 17% of the total population of one of the two null mutants of LmxMPK3 (mutant Δ2), having an average flagellar length of about 6.7 μm, show normal PFR architecture (18). However, this argument can be downplayed through two separate studies, one on the same SMP-1 protein where cells treated with myriosin and ketoconazole bore a very short axoneme (54) and the other on null mutants of the outer dynein arm-docking complex (LdDC2), having mean flagellar lengths of 3.7 μm and 2.9 μm (26). In both these instances the PFR is fully assembled. Clearly, more studies are required to dissect the mechanisms that correlate the axoneme assembly with the PFR assembly.

One distinct feature of the S4D-overexpressing cells is that these cells are stumpy with small flagella, morphologically similar to ADF/cofilin gene knockout mutants (52), myosin XXI heterozygous gene deletion mutants (33), and many other flagellar mutants (2, 16, 18, 26, 53, 56), including a recently reported dysflagellar strain of *L. braziliensis* (59). Based on these studies, we envisage that like in *Trypanosoma brucei* (1, 35), a correlation may exist between the flagellar length and the cell body length. However, this appears to be untenable, because unlike the *Trypanosoma* flagellum, which is physically attached to the cell body through the flagellar attachment zone, the *Leishmania* flagellum is largely free, and there is no clear evidence to relate the flagellar length to the cell body length. Moreover, the flagellar length has been shown to vary in different growth stages of *Leishmania* promastigotes in culture, with 3-fold differences between the flagellar lengths of early-log-phase and stationary-phase parasites (33). In addition, overexpression of the microtubule-depolymerizing kinesin in *Leishmania* leads to the short flagellar phenotype with no significant effect on the cell body length (9). Interestingly, all the flagellar mutants that have short flagella with a stumpy shape are nonmotile, whereas others, such as early-log-phase cells or kinesin-overexpressing cells, are fully motile. Since the motile cells retain their spindle shape despite having shorter flagella and the nonmotile cells are invariably short and stumpy, we hypothesize that cell motility is the key factor that maintains the cell shape.

Our results show that dynamic actin is essentially required in flagellum assembly, especially in the assembly of the PFR and the axoneme attachment fibers. It further indicates that dynamic actin may also play a role in axoneme assembly. Based on these and our earlier observations (33, 52), we infer that the actin-based myosin motor function is essentially required in the PFR assembly and also in the assembly of the axoneme fibers. In addition, we suggest that this motor function might also be required in the axoneme assembly. Finally, it is proposed that an intimate cross talk between the IFT and the actin-based myosin motor activities is perhaps required in the assembly of the eukaryotic flagellum.

ACKNOWLEDGMENTS

This work was supported by a research grant awarded to C.M.G. by the Department of Biotechnology, Government of India, New Delhi, India, under the Distinguished Biotechnology Research Professor Award Scheme. We also acknowledge funding from the Council of Scientific and Industrial Research (grant NWP0038). G.K. is a recipient of a Research Fellowship from the Council of Scientific and Industrial Research, Rafi Marg, New Delhi, India.

REFERENCES

1. **Absalon S, et al.** 2008. Intraflagellar transport and functional analysis of genes required for flagellum formation in trypanosomes. Mol. Biol. Cell **19**:929–944.
2. **Adhiambo C, Forney JD, Asai DJ, LeBowitz JH.** 2005. The two cytoplasmic dynein-2 isoforms in Leishmania mexicana perform separate functions. Mol. Biochem. Parasitol. **143**:216–225.
3. **Agnew BJ, Minamide LS, Bamburg JR.** 1995. Reactivation of phosphorylated actin depolymerizing factor and identification of the regulatory site. J. Biol. Chem. **270**:17582–17587.
4. **Bastin P.** 2010. The peculiarities of flagella in parasitic protozoa. Curr. Opin. Microbiol. **13**:450–452.
5. **Baumgartner M.** 2011. Enforcing host cell polarity: an apicomplexan parasite strategy towards dissemination. Curr. Opin. Microbiol. **14**:436–444.
6. **Bernard O.** 2007. Lim kinases, regulators of actin dynamics. Int. J. Biochem. Cell Biol. **39**:1071–1076.
7. **Bernstein BW, Bamburg JR.** 2010. ADF/cofilin: a functional node in cell biology. Trends Cell Biol. **20**:187–195.
8. **Betleja E, Cole DG.** 2010. Ciliary trafficking: CEP290 guards a gated community. Curr. Biol. **20**:R928–R931.
9. **Blaineau C, et al.** 2007. A novel microtubule-depolymerizing kinesin involved in length control of a eukaryotic flagellum. Curr. Biol. **17**:778–782.
10. **Bouyer S,. Rodier MH, Guillot A, Hechard Y.** 2009. *Acanthamoeba castellanii*: proteins involved in actin dynamics, glycolysis, and proteolysis are regulated during encystation. Exp. Parasitol. **123**:90–94.
11. **Bugyi B, Carlier MF.** 2010. Control of actin filament treadmilling in cell motility. Annu. Rev. Biophys. **39**:449–470.
12. **Carlier MF, et al.** 1997. Actin depolymerizing factor (ADF/cofilin) enhances the rate of filament turnover: implication in actin-based motility. J. Cell Biol. **136**:1307–1322.
13. **Cevallos AM, et al.** 2011. *Trypanosoma cruzi*: multiple actin isovariants are observed along different developmental stages. Exp. Parasitol. **127**:249–259.
14. **Cole DG.** 2003. The intraflagellar transport machinery of *Chlamydomonas reinhardtii*. Traffic **4**:435–442.
15. **Cramer L.** 2008. Organelle transport: dynamic actin tracks for myosin motors. Curr. Biol. **18**:1066–1068.
16. **Cuvillier A, Miranda JC, Ambit A, Barral A, Merlin G.** 2003. Abortive infection of Lutzomyia longipalpis insect vectors by aflagellated LdARL-3A-Q70L overexpressing Leishmania amazonensis parasites. Cell. Microbiol. **5**:717–728.
17. **Davidge JA, et al.** 2006. Trypanosome IFT mutants provide insight into the motor location for mobility of the flagella connector and flagellar membrane formation. J. Cell Sci. **119**:3935–3943.
18. **Erdmann M, Scholz A, Melzer IM, Schmetz C, Wiese M.** 2006. Interacting protein kinases involved in the regulation of flagellar length. Mol. Biol. Cell **17**:2035–2045.
19. **Ersfeld K, Gull K.** 2001. Targeting of cytoskeletal proteins to the flagellum of *Trypanosoma brucei*. J. Cell Sci. **114**:141–148.
20. **Fowkes ME, Mitchell DR.** 1998. The role of preassembled cytoplasmic complexes in assembly of flagellar dynein subunits. Mol. Biol. Cell **9**:2337–2347.
21. **Garcia-Salcedo JA, et al.** 2004. A differential role for actin during the life cycle of *Trypanosoma brucei*. EMBO J. **23**:780–789.
22. **Gluenz E, Ginger ML, McKean PG.** 2010. Flagellum assembly and function during the *Leishmania* life cycle. Curr. Opin. Microbiol. **13**:473–479.
23. **Gonzalez-Robles A, et al.** 2008. *Acanthamoeba castellanii*: identification and distribution of actin cytoskeleton. Exp. Parasitol. **119**:411–417.
24. **Goode BL, Drubin DG, Barnes G.** 2000. Functional cooperation between the microtubule and actin cytoskeletons. Curr. Opin. Cell Biol. **12**:63–71.
25. **Gull K.** 1999. The cytoskeleton of trypanosomatid parasites. Annu. Rev. Microbiol. **53**:629–655.
26. **Harder S, Thiel M, Clos J, Bruchhaus I.** 2010. Characterization of a subunit of the outer dynein arm docking complex necessary for correct flagellar assembly in *Leishmania* donovani. PLoS Negl. Trop. Dis. **4**:e586. doi:10.1371/journal.pntd.0000586.
27. **Hu Q, Nelson WJ.** 2011. Ciliary diffusion barrier: the gatekeeper for the primary cilium compartment. Cytoskeleton (Hoboken, N.J.) **68**:313–324.
28. **Ishikawa H, Marshall WF.** 2011. Ciliogenesis: building the cell's antenna. Nat. Rev. Mol. Cell Biol. **12**:222–234.

29. **Ismach R, et al.** 1989. Flagellar membrane and paraxial rod proteins of *Leishmania*: characterization employing monoclonal antibodies. J. Protozool. **36**:617–624.
30. **Kapoor P, et al.** 2008. An unconventional form of actin in protozoan hemoflagellate, *Leishmania.* J. Biol. Chem. **283**:22760–22773.
31. **Kato-Minoura T.** 2005. Impaired flagellar regeneration due to uncoordinated expression of two divergent actin genes in *Chlamydomonas.* Zoolog. Sci. **22**:571–577.
32. **Katta SS, Sahasrabuddhe AA, Gupta CM.** 2009. Flagellar localization of a novel isoform of myosin, myosin XXI, in *Leishmania.* Mol. Biochem. Parasitol. **164**:105–110.
33. **Katta SS, Tammana TV, Sahasrabuddhe AA, Bajpai VK, Gupta CM.** 2010. Trafficking activity of myosin XXI is required in assembly of *Leishmania* flagellum. J. Cell Sci. **123**:2035–2044.
34. **Kim J, et al.** 2010. Functional genomic screen for modulators of ciliogenesis and cilium length. Nature **464**:1048–1051.
35. **Kohl L, Bastin P.** 2005. The flagellum of trypanosomes. Int. Rev. Cytol. **244**:227–285.
36. **Maga JA, Sherwin T, Francis S, Gull K, LeBowitz JH.** 1999. Genetic dissection of the *Leishmania* paraflagellar rod, a unique flagellar cytoskeleton structure. J. Cell Sci. **112**:2753–2763.
37. **Mullin KA, et al.** 2001. Regulated degradation of an endoplasmic reticulum membrane protein in a tubular lysosome in *Leishmania mexicana.* Mol. Biol. Cell **12**:2364–2377.
38. **Muto E, Edamatsu M, Hirono M, Kamiya R.** 1994. Immunological detection of actin in the 14S ciliary dynein of *Tetrahymena.* FEBS Lett. **343**:173–177.
39. **Nayak RC, Sahasrabuddhe AA, Bajpai VK, Gupta CM.** 2005. A novel homologue of coronin colocalizes with actin in filament-like structures in *Leishmania.* Mol. Biochem. Parasitol. **143**:152–164.
40. **Ono S.** 2007. Mechanism of depolymerization and severing of actin filaments and its significance in cytoskeletal dynamics. Int. Rev. Cytol. **258**: 1–82.
41. **Pardee JD, Spudich JA.** 1982. Purification of muscle actin. Methods Enzymol. **85**:164–181.
42. **Portman N, Gull K.** 2010. The paraflagellar rod of kinetoplastid parasites: from structure to components and function. Int. J. Parasitol. **40**:135–148.
43. **Qin H, Diener DR, Geimer S, Cole DG, Rosenbaum JL.** 2004. Intraflagellar transport (IFT) cargo: IFT transports flagellar precursors to the tip and turnover products to the cell body. J. Cell Biol. **164**:255–266.
44. **Ralston KS, Hill KL.** 2008. The flagellum of *Trypanosoma brucei*: new tricks from an old dog. Int. J. Parasitol. **38**:869–884.
45. **Rodionov VI, Hope AJ, Svitkina TM, Borisy GG.** 1998. Functional coordination of microtubule-based and actin-based motility in melanophores. Curr. Biol. **8**:165–168.
46. **Rogers SL, Gelfand VI.** 1998. Myosin cooperates with microtubule motors during organelle transport in melanophores. Curr. Biol. **8**:161–164.
47. **Sahasrabuddhe AA, Bajpai VK, Gupta CM.** 2004. A novel form of actin in *Leishmania*: molecular characterisation, subcellular localisation and association with subpellicular microtubules. Mol. Biochem. Parasitol. **134**: 105–114.
48. **Sahin A, et al.** 2008. The *Leishmania* ARL-1 and Golgi traffic. PLoS One **3**:e1620. doi:10.1371/journal.pone.0001620.
49. **Schuler H, Matuschewski K.** 2006. Regulation of apicomplexan microfilament dynamics by a minimal set of actin-binding proteins. Traffic **7**:1433–1439.
50. **Semenova I, et al.** 2008. Actin dynamics is essential for myosin-based transport of membrane organelles. Curr. Biol. **18**:1581–1586.
51. **Tammana TV, Sahasrabuddhe AA, Bajpai VK, Gupta CM.** 2010. ADF/cofilin-driven actin dynamics in early events of *Leishmania* cell division. J. Cell Sci. **123**:1894–1901.
52. **Tammana TV, Sahasrabuddhe AA, Mitra K, Bajpai VK, Gupta CM.** 2008. Actin-depolymerizing factor, ADF/cofilin, is essentially required in assembly of *Leishmania* flagellum. Mol. Microbiol. **70**:837–852.
53. **Tull D, et al.** 2010. Membrane protein SMP-1 is required for normal flagellum function in *Leishmania.* J. Cell Sci. **123**:544–554.
54. **Tull D, et al.** 2004. SMP-1, a member of a new family of small myristoylated proteins in kinetoplastid parasites, is targeted to the flagellum membrane in *Leishmania.* Mol. Biol. Cell **15**:4775–4786.
55. **Watanabe Y, Hayashi M, Yagi T, Kamiya R.** 2004. Turnover of actin in *Chlamydomonas* flagella detected by fluorescence recovery after photobleaching (FRAP). Cell Struct. Funct. **29**:67–72.
56. **Wiese M, Kuhn D, Grünfelder CG.** 2003. Protein kinase involved in flagellar-length control. Eukaryot. Cell **2**:769–777.
57. **Wolfrum U, Liu X, Schmitt A, Udovichenko IP, Williams DS.** 1998. Myosin VIIa as a common component of cilia and microvilli. Cell Motil. Cytoskeleton **40**:261–271.
58. **Yanagisawa HA, Kamiya R.** 2001. Association between actin and light chains in *Chlamydomonas* flagellar inner-arm dyneins. Biochem. Biophys. Res. Commun. **288**:443–447.
59. **Zauli RC, et al.** 2012. A dysflagellar mutant of *Leishmania* (Viannia) braziliensis isolated from a cutaneous leishmaniasis patient. Parasit. Vectors **5**:11.
60. **Zheng M, et al.** 2009. Actin turnover is required for myosin-dependent mitochondrial movements in *Arabidopsis* root hairs. PLoS One **4**:e5961. doi:10.1371/journal.pone.0005961.